MITIGATING NEW YORK CITY'S HEAT ISLAND

Integrating Stakeholder Perspectives and Scientific Evaluation

BY CYNTHIA ROSENZWEIG, WILLIAM D. SOLECKI, LILY PARSHALL, BARRY LYNN, JENNIFER COX, RICHARD GOLDBERG, SARA HODGES, STUART GAFFIN, RONALD B. SLOSBERG, PETER SAVIO, FRANK DUNSTAN, AND MARK WATSON

Heat island mitigation benefits from the collaboration between researchers and stakeholders, interdisciplinary methods, and neighborhood-scale strategies that account for local priorities and constraints.

The urban heat island effect[1] can be detected throughout the year, but it is of particular public policy concern during the summer, because higher surface air temperature is associated with increases in electricity demand for air conditioning, air pollution, and heat stress–related mortality and illness (Rosenfeld et al. 1995; Nowak et al. 2000; Sailor et al. 2002; Hogrefe et al. 2004). In New York City, New York (NYC), the heat island impacts interact with aging energy and water infrastructure and the anticipated regional effects of global climate change. This has led local decision makers to ask whether heat island mitigation can help to address some of these related urban challenges, for example, by reducing electricity demand for cooling, absorbing stormwater runoff, and reducing the health impacts of heat waves.

Our main goal was to compare the possible effectiveness of heat island mitigation strategies to increase urban vegetation, such as planting trees or incorporating vegetation into rooftops, with strategies to increase the albedo of impervious surfaces. The specific stakeholder question guiding our research was the following: can heat island mitigation strategies reduce peak electricity demand in neighborhoods with potential electric distribution constraints

[1] Urbanization is often associated with elevated surface air temperature, a condition referred to as the urban heat island. Aspects of the urban environment that contribute to the urban heat island include i) dense, impervious surfaces that reduce evaporative latent heat cooling and increase the amount of energy that is absorbed and stored in the city; ii) low-albedo surfaces, such as dark rooftops and asphalt roadways; iii) reduced skyview from within urban canyons, which impedes radiative longwave cooling to space, a process that is especially important at night (Oke 1981); and iv) anthropogenic heat sources associated with transportation and building heating and cooling systems (Taha 1997; Hsieh et al. 2007). Heat island intensity tends to be greatest at night, particularly when conditions are clear and calm. Local hot spots may shift with diurnal and seasonal cycles, under particular meteorological conditions, or with land use change (Unwin 1980). Landsberg (1981) and Oke (1987) describe urban climate and heat island processes. More recent reviews can be found in Arnfield (2003) and Grimmond (2007).

(known as load pockets)? Therefore, key stakeholders included Con Edison, the local utility responsible for the majority of electricity and gas distribution in New York City, and the New York State Energy Research and Development Authority (NYSERDA).

The broad range of links between heat island mitigation and other local environmental policy goals provided an opportunity to bring together stakeholders—principally city and state agencies—with an interest in understanding how their specific mandates and priorities might overlap with the objectives that NYSERDA and Con Edison hoped to achieve through heat island mitigation.[2] For example, the New York State Department of Environmental Conservation (NYSDEC) was interested in urban greening programs that could improve the quality of life in low-income, high-minority neighborhoods.

Therefore, when we selected case study neighborhoods, we used a geographic information system (GIS) to look for overlap between neighborhoods Con Edison was concerned about from an electricity perspective and neighborhoods that the NYSDEC was concerned about from an environmental equity perspective. We also incorporated other factors into the GIS system; for example, we worked with the New York City Department of Parks (Parks Department) to identify neighborhoods with available space to plant additional street trees. The Parks Department was interested in our study results because heat island mitigation is among the suite of factors often cited in support of urban forestry programs in New York City neighborhoods.

We used the fifth-generation Pennsylvania State University (PSU)–National Corporation for Atmospheric Research (NCAR) Mesoscale Model (MM5) to compare the effectiveness of each of the mitigation strategies in the selected case study neighborhoods. Our stakeholders played a key role in helping us to "localize" our representation of the strategies in the model. For example, the Department of Design and Construction helped us to select an appropriate albedo for "high albedo" surfaces based on roofing and paving materials that are commercially available in the New York area. The Parks Department shared a detailed database on the number of existing trees, as well as the number of new trees that could be planted, along each individual street segment; provided information on the typical canopy size of mature trees planted in New York; and helped us to understand which types of open, vegetated space with additional trees could be added; for example, small, pocket parks could be planted, but playgrounds and gardens could not.

Our energy stakeholders considered a strategy to be "effective" if it could reduce the temperature of air entering buildings through ventilation and infiltration, the primary determinant of air-conditioning loads.[3] In the observed meteorological record, this is best represented by the surface air temperature. In our simulations, we evaluate heat island mitigation strategies by testing their possible effectiveness at reducing *urban air temperature*. We define urban air temperature as a weighted average of simulated 2-m air temperature and radiative surface temperature (skin temperature of exposed surfaces). The designation of urban air temperature encompasses the effect of a heterogeneous mix of land surface cover, including variation in the height of built surfaces and vegetation, on surface air temperature within the urban canopy layer.

AFFILIATIONS: Rosenzweig—NASA Goddard Institute for Space Studies, New York, New York; Solecki, Cox, and Hodges—Geography Department, Hunter College—CUNY, New York, New York; Parshall, Lynn, Goldberg, and Gaffin—Center for Climate Systems Research, Columbia University, New York, New York; Slosberg—L & S Energy Services, Clifton Park, New York; Savio and Watson—New York State Energy Research and Development Authority, Albany, New York; Dunstan—New York State Department of Environmental Conservation, Albany, New York

CORRESPONDING AUTHOR: Cynthia Rosenzweig, Goddard Institute for Space Studies, 2880 Broadway, New York, NY 10025
E-mail: crosenzweig@giss.nasa.gov

The abstract for this article can be found in this issue, following the table of contents.
DOI:10.1175/2009BAMS2308.1

In final form 22 December 2008

[2] The project was sponsored by NYSERDA and the New York State Department of Environmental Conservation (NYSDEC). The research team met regularly with NYSERDA and NYSDEC to refine research questions and receive feedback on research approaches, and with a steering group from local and national government agencies including NYC Department of Parks and Recreation, NYC Department of Design and Construction, and U.S. Environmental Protection Agency (EPA) Region II], nongovernmental organizations (e.g., Sustainable Energy Partnerships and Environmental Energy Alliance of New York), and private utilities (e.g., Con Edison).

[3] A secondary determinant of energy demand for cooling is conductive heat flow through building roofs and walls. Reductions in the temperature of building surfaces can reduce conductive heat flow.

NEW YORK CITY'S HEAT ISLAND. Surface air temperatures elevated by at least 1°C have been observed in New York City for more than a century (Rosenthal et al. 2003; Gaffin et al. 2008), and the heat island signal, measured as the difference between the urban core and the surrounding rural surface air temperature readings taken at National Weather Service (NWS) stations, averages ~4°C on summer nights (Kirkpatrick and Shulman 1987; Gedzelman et al. 2003; Gaffin et al. 2008). The greatest temperature differences typically are sustained between midnight and 0500 Eastern Standard Time (EST; Gaffin et al. 2008).

Surface air temperature data from weather stations both in and around New York City were mapped to show the heat island at 0600 EST 14 August 2002, the early morning of what would become one of the hottest heat-wave days that summer (Fig. 1). Within the city, the three NWS stations are located in Central Park, and at LaGuardia and John F. Kennedy airports. To improve coverage of New York City, data were obtained from the WeatherBug network of automated private stations (AWS; online at www.aws.com/aws_2005/default.asp).[4] Surface air temperature readings from these stations show that the city was several degrees warmer than the suburbs, and up to 8°C warmer than rural areas within 100 km of the city, with conditions that had been sustained throughout the previous night. These data confirm that New York City's heat island can be particularly

[4] There is less uniformity in the WeatherBug data relative to the NWS sites because some WeatherBug stations are placed on rooftops, and thus stations are located at various heights. A comparison of WeatherBug data with NWS air temperature, sea level pressure, relative humidity, and wind data showed that, with the exception of the station representing Lower Manhattan East, WeatherBug readings are reasonably accurate.

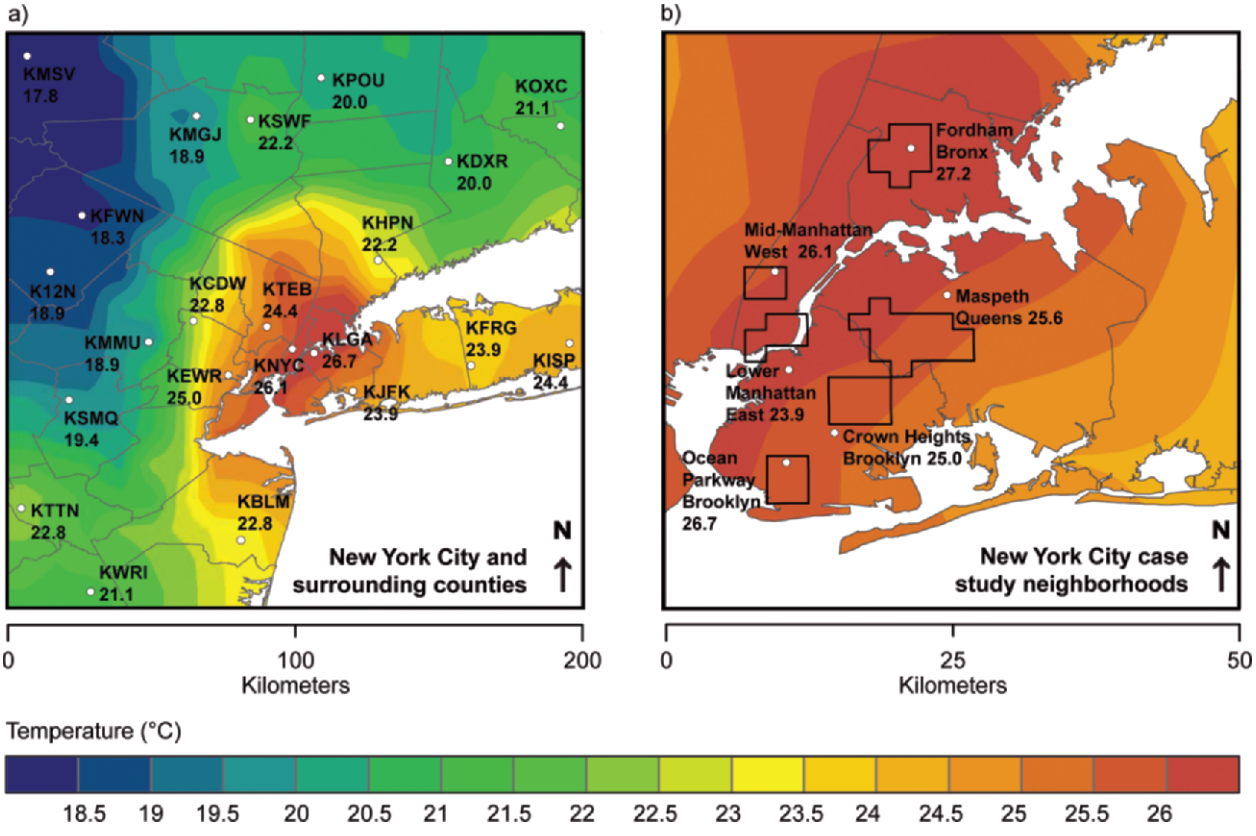

Fig. 1. New York City's urban heat island at 0600 EST 14 Aug 2002 based on surface air temperature readings taken at NWS and WeatherBug stations. (a) New York City and surrounding counties, with locations of NWS stations. (b) New York City case study neighborhoods, with locations of WeatherBug stations. Note: Inverse-weighted-distance interpolation with three neighbors, a power value of 1, a variable search radius, and an output grid size of 0.1° were applied to meteorological data. All NWS and WeatherBug data shown were used in the interpolation, with the exception of the WeatherBug station representing Lower Manhattan East, which was excluded because of low confidence in data quality. Because multiple neighboring points contributed to the interpolation, contours may differ from individual station temperatures.

pronounced during heat wave conditions, which are often characterized by low wind speed, in addition to high temperature (Rosenzweig et al. 2005).

The archipelago-like structure of the heat island was also apparent, with differences of more than 2°C recorded by NWS and WeatherBug stations located in neighborhoods around the city. Some of these differences can be related to a variation in surface heating at the beginning of the night. For example, mid-Manhattan stands out as having higher radiative surface temperatures in the evening than other parts of the city, which is most likely a result of a reduced sky view associated with taller buildings (Fig. 2).[5] As the previous night's heat island dissipates with early morning solar radiation throughout the region, the process of surface heating repeats. Areas like mid-Manhattan that have deep, shaded canyons heat up more slowly than the exposed expanses of flat, dark roofs and asphalt roadways in northwestern Brooklyn, eastern Queens, and the South Bronx, a pattern observed during other seasons as well (Childs and Raman 2005). This highlights the importance of a neighborhood-scale approach to evaluating mitigation strategies.

URBAN HEAT ISLAND MITIGATION STRATEGIES. Three possible urban heat island mitigation strategies are urban forestry, green roofs, and high-albedo surfaces. These strategies can directly lower surface temperature through shading, evapotranspiration, and reflection of radiation (Taha 1997), and they can reduce conductive heat flow into buildings. Reduced radiative surface temperatures also lower the sensible heat fluxes from the ground during the day and the amount of heat stored in urban surfaces at night, both of which can lower urban air temperature. This in turn reduces the temperature of air entering buildings through ventilation and infiltration, a key factor in air-conditioning loads.

Urban forestry refers to planting trees in open spaces where they shade grass, or along streets where they shade impervious surfaces. In a previous study of New York City, Luley and Bond (2002) simulated the impact of increasing tree cover on surface air temperature. In their maximum scenario, in which all urban grass is replaced with trees, surface air temperature is reduced by up to 1°C on a summer afternoon, with greater reductions downwind of Manhattan (Luley and Bond 2002). Another modeling study of the Northeast United States demonstrated that increasing tree cover by approximately 40% in three urban areas—New York City, Philadelphia, Pennsylvania; and Baltimore, Maryland—reduced urban surface air temperature by as much as 6°C, with more typical reductions on the order of 1°–2°C (Civerolo et al. 2000; Nowak et al. 2000). In addition to reducing

[5] An analysis of radiative surface temperature is based on remotely-sensed satellite data from 8 September 2002 rather than 14 August 2002 because data were not available for 14 August. Patterns of surface heating are expected to be similar on these 2 days, although the magnitude of radiative surface temperatures would be different.

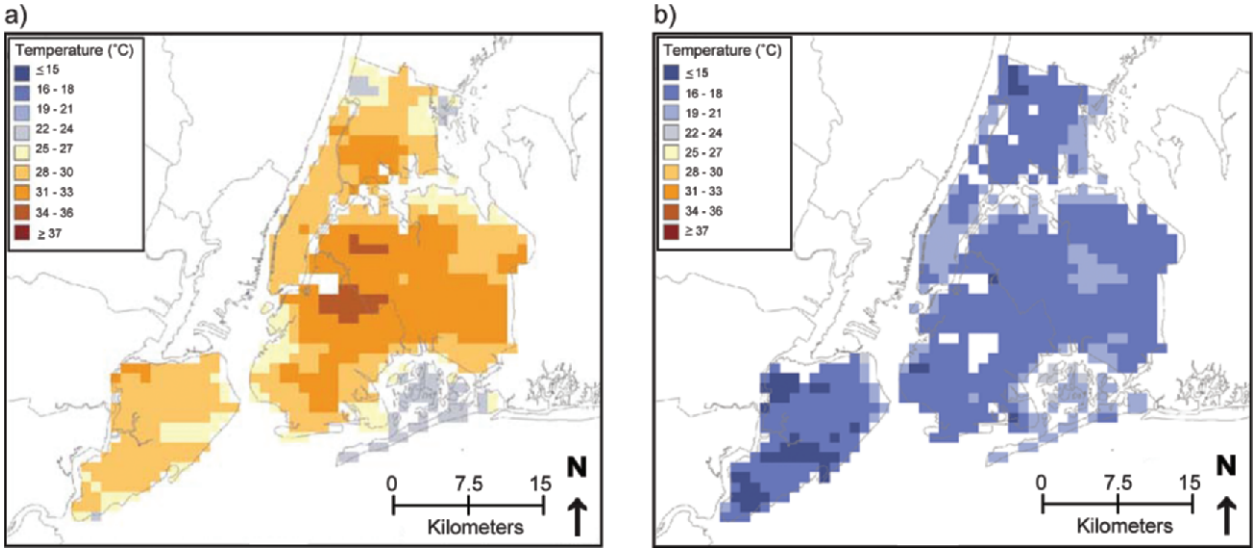

FIG. 2. New York City radiative surface (skin) temperature: 1030 EST 8 Sep 2002 and (b) 2230 EST 8 Sep 2002. Note: Data were extracted from remotely-sensed MODIS land surface temperature and emissivity daily L3 global data using a view-angle-dependent algorithm. Spatial resolution is 1 km.

surface air temperature, trees can also directly reduce energy demand through shading windows and built surfaces (Davis et al. 1992), and they can improve air quality through the direct uptake of pollutants [as long as they are not high emitters of volatile organic compounds; Taha (1996)].

Green roofs cover a building's upper surface with vegetation, cooling the roof through evapotranspiration and shading. Modern green roofs tend to be thin, lightweight systems planted with hardy, drought-resistant plants to minimize weight, cost, and maintenance. A study in Toronto, Ontario, Canada, showed that adding green roofs in 50% of the available space could reduce surface air temperature by 0.1°–0.8°C, without irrigation, and up to 2°C with irrigation (Bass et al. 2003). By moderating the flow of heat into and out of buildings, green roofs can also directly reduce energy demand, and by retaining, evaporating, and delaying runoff, they can reduce stormwater-runoff pollution, which is another impact of urbanization (Rosenzweig et al. 2006a). In a city with limited space for street-level planting, green roofs can provide an opportunity to reintroduce vegetation.

High-albedo surfaces can reduce the absorption of radiation. For example, pavements can be made more reflective through the use of lighter-colored aggregate in asphalt or of other resurfacing material, or through substituting concrete for asphalt (Davis et al. 1992). A case study of Los Angeles showed that increasing citywide albedo by 15% could reduce surface air temperature in the downtown area by up to 2°C in the midafternoon (Taha et al. 1997). The major advantages of high-albedo surfaces are a large available area for implementation (e.g., impervious streets, sidewalks, and roofs) and a relatively low cost per unit area. However, high-albedo surfaces may lose up to one-third of their reflectivity in a few years (Bretz and Pon 1994), and they often scatter radiation to other surfaces. Recent research has demonstrated the potential for significant cooling from nonwhite, near-infrared reflective architectural coatings, which may have greater consumer appeal (Levinson et al. 2007).

As heat island mitigation has become part of the urban policy agenda, there have been an increasing number of efforts to compare strategies and their impacts. The U.S. EPA's Heat Island Reduction Initiative has supported mesoscale modeling of urban meteorology and heat island mitigation scenarios in a number of U.S. cities, including Los Angeles, California; Phoenix, Arizona; Washington, D.C.; Atlanta, Georgia; and New Orleans, Louisiana (U.S. EPA 2007).

CASE STUDY NEIGHBORHOODS. We selected six neighborhoods for analysis of heat island mitigation: Mid-Manhattan West, Lower Manhattan East, Fordham Bronx, Maspeth Queens, Crown Heights Brooklyn, and Ocean Parkway Brooklyn (see Fig. 1). We used several selection criteria agreed upon with stakeholders: 1) location within an area with potential electric distribution constraints (anticipated possible load pocket), as defined by Con Edison; 2) measurement of warmer-than-average surface air temperatures (i.e., a "hot spot"); and 3) presence of an available area for testing a range of heat island mitigation strategies. In addition, we included some low-income and minority neighborhoods so that the results could be used to address environmental equity concerns. All case study areas met the criteria, with the exception of Lower Manhattan, which is not in a designated load pocket. Crown Heights and Fordham are low-income, high-minority neighborhoods.

Two case study neighborhoods illustrate the extent to which neighborhoods within New York City can differ in their land use and other aspects of the built environment: Mid-Manhattan West and Maspeth Queens (Fig. 3). Mid-Manhattan West, located in western Manhattan from 35th Street to the southern end of Central Park at 59th Street, is approximately 7 km^2 running along the coast of the Hudson River. The central portion of this area is a commercial and business district with high-rise buildings, street-level commercial space, and very few vegetated areas. The daytime working population is much higher than the residential population.

The Maspeth Queens case study area, located in west-central Queens, is 29 km^2 and has pockets of lower radiative surface temperatures in Forest Park and other large, vegetated areas (see Fig. 3). The neighborhood contains a large industrial area, many cemeteries, and several residential areas with a mix of detached homes and high-rise apartment buildings.

Many characteristics of individual neighborhoods affect the potential for heat island mitigation strategies to reduce electricity demand for cooling. These include the available area for implementing each strategy, the extent to which each strategy may be able to reduce surface air temperature, and the extent to which reductions in surface air temperature may reduce electricity demand. In addition to vegetation and albedo, building geometry and material can affect surface air temperature, and building design and use can affect the sensitivity of electricity demand to changes in surface air temperature. Our data library contains a wide range of variables relevant to

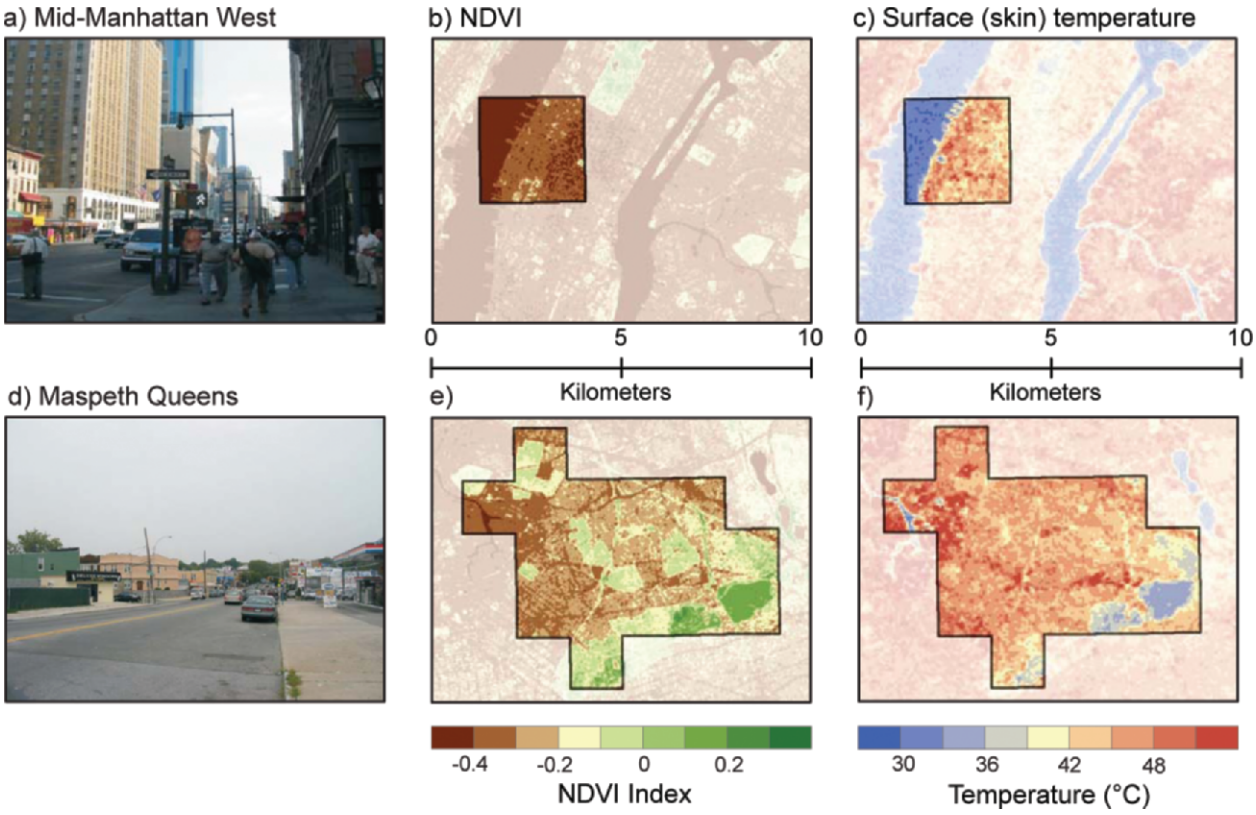

Fig. 3. Characteristics of two of the case study neighborhoods: (a)–(c) Mid-Manhattan West and (d)–(f) Maspeth, Queens. Note: NDVI was derived from *Landsat*-7 10:30 EST 8 Sep 2002 30-m-resolution data and computed using red and near-infrared (nir) bands. NDVI = (nir – red)/(nir + red). Units are nondimensional, with a range from –1 to 1, with higher values indicating greater vegetation intensity. Radiative surface (skin) temperature was derived from *Landsat*-7 1030 EST 14 Aug 2002 60-m-resolution data and computed based on methods described in Voogt and Oke (2003) and Aniello et al. (1995).

understanding the many factors that affect heat island mitigation in New York (see the appendix).

REGIONAL CLIMATE MODEL. We used a modified version of the MM5 regional climate model version 3.7 to simulate the impact of the heat island mitigation strategies on urban air temperature in the city as a whole and in each of the case study areas (Lynn et al. 2009). MM5 is a three-dimensional nonhydrostatic model that dynamically simulates the interactions among a range of land surface cover and climate variables (Dudhia 1993; Grell et al. 1994). The model was run over an eastern U.S. domain at 36 km with progressively smaller nests at 12, 4, and 1.3 km (Fig. 4a). The Medium Range Forecast (MRF) physics scheme was used, which includes both local and nonlocal mixing, and turbulence was parameterized using first-order closure. Radiative surface temperature was initialized within the model.

To improve the ability of MM5 to simulate air temperature in an urban setting, the land surface within each 1.3-km grid cell was modeled with four tiles representing impervious surfaces, grass, trees, and water, respectively. A 1.3-km resolution was chosen to obtain variation at the scale of an urban neighborhood. Within the New York City study area, the amount of each type of surface was derived from a land surface cover database developed following the methods described in Myeong et al. (2001), using Emerge® infrared aerial photography obtained from flyovers during 2001 (OASIS 2001). Land surface cover data available at 3-m resolution were summed to the 1.3-km MM5 grid cells. The percentage of each MM5 grid cell that is covered with each land surface cover type is shown in Fig. 4b–d. Between the surface and the first layer of the model, air temperatures for each type of surface cover were computed using a local roughness length for each tile. The fluxes from the tiles were then aggregated in the first layer of the model. Although buildings are not explicitly represented in the model, their presence is assumed through the boundary layer structure, which controls the surface transport of heat and moisture (Grimmond and Oke 1999).

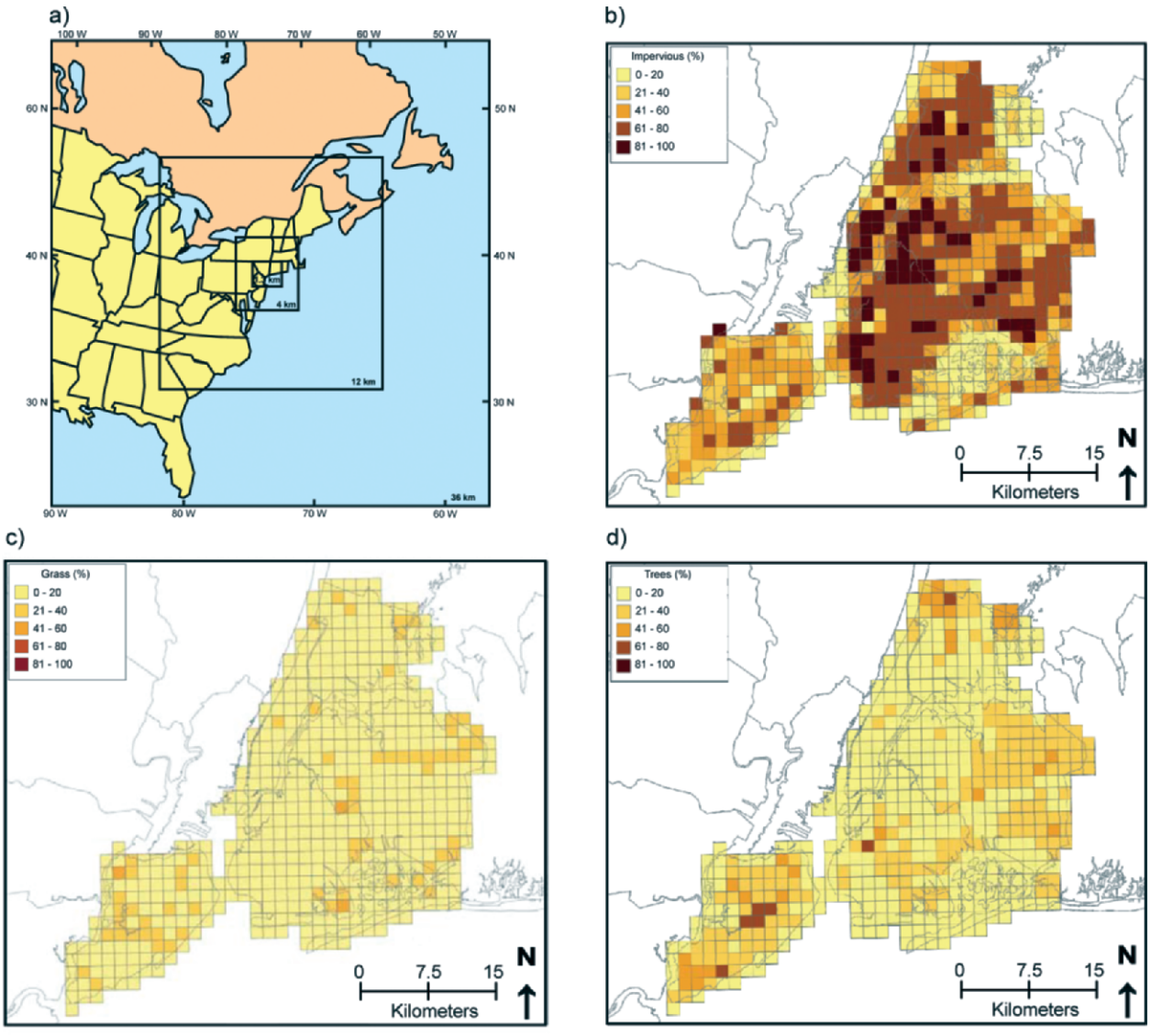

Fig. 4. Land surface cover specification for MM5 grid cells derived from New York City land cover classification by Myeong et al. (2001). Original data at 3-m resolution were aggregated to 1.3-km grid cells. See the appendix for more information about the underlying data. (a) MM5 domain for 36-, 12-, 4-, and 1.3-km nests. (b) Percentage of each grid cell with impervious land surface cover. (c) Percentage of each grid cell with grass land surface cover. (d) Percentage of each grid cell with tree land surface cover.

This was represented by a global urban roughness of 1 m, applied uniformly citywide (Pielke 2001; Lynn et al. 2009). This roughness length was chosen based on a nominal building height of 10 m, which is common in New York City outside the borough of Manhattan, with the assumption that roughness length should be approximately equal to one-tenth of the building height.

The surface energy balance for each type of land surface cover was based on a modified version of the National Oceanic and Atmospheric Administration (NOAA) Land Surface Model (LSM) that better represents the urban environment (Chen and Dudhia 2001a,b; Liu et al. 2006). Liu et al. found that their model could simulate the first-order effects of urbanization reasonably well without incorporating the more advanced urban canopy models described in, for example, Otte et al. (2004). Key land surface modifications incorporated by Liu et al. (2006) include a reduced surface albedo to account for the trapping of shortwave radiation in urban canyons, an increase in volumetric heat capacity and soil thermal conductivity above values that are typically assigned to concrete and asphalt to reflect heat storage in building walls, and a reduction in the green vegetation fraction and soil water capacity to reflect reduced

evaporation. The parameters we use to describe each type of land surface cover are shown in Table 1.

Outside of the New York City study area, standard U.S. Geological Survey (USGS) land surface cover data were used, and cells were not subdivided into tiles (Brown et al. 1993). For grid cells representing grass and trees, vegetation fraction intensity (a measure of the intensity of vegetative processes such as photosynthesis) was specified according to a vegetated fraction dataset described in Small (2001).[6]

MM5 runs covered three heat-wave periods during the summer of 2002: 2–4 July (HWI), 28 July–7 August (HW2), and 11–18 August (HW3; Fig. 5). The NWS defines a heat wave as at least three consecutive days with maximum surface air temperatures above 32.2°C (NYC Office of Emergency Management 2008). The three heat-wave periods were identified using NWS data from Central Park. Heat-wave periods were chosen because the need for heat island mitigation is greater during episodes of prolonged elevated temperature.

Initially, simulated 2-m air temperatures were compared to observed NWS data from Central Park, and at La Guardia and John F. Kennedy airports. However, after noting that observed surface air temperatures tended to fall between 2-m and radiative surface temperatures simulated by MM5, we concluded that MM5 was not fully capturing the effect of the urban environment on surface air temperature. In the model, regional meteorology seemed to be dominating local microclimates influenced by surface heating; to address this, a weighting function was derived. Based on RMSE optimization across all heat-wave days and case study areas, we arrived at the following function: $T_{\text{MM5 urban air}} = 0.3^{*}T_{\text{MM5 surface}} + 0.7^{*}T_{\text{MM5 2-meter air}}$. We refer to this simulated temperature as urban air temperature.

MM5 simulations were evaluated by comparing simulated base data to observed meteorological data from NWS and WeatherBug stations. At Central Park, the average error for the third heat wave is 1.0°C, the RMSE is 1.7°C, and the correlation is 0.94 (Fig. 6). The RMSE at Central Park is higher in the first and second heat waves (2.3° and 2.2°C, respectively), mainly because the timing of the simulated urban air temperature peaks and troughs do not match up as well with the observed surface air temperature. There are larger errors at John F. Kennedy airport because of problems with the simulation of sea breezes in MM5. The RMSE for the WeatherBug stations tends to be within the range of values reported for the NWS stations, although a lack of uniformity in the siting of stations can affect data quality.

Simulated heat island mitigation scenarios. We selected six mitigation scenarios to test with MM5 for NYC as a whole and for the six case study areas: 1) planting trees in grassy open spaces such as parks; 2) planting trees along streets; 3) green roofs; 4) a combination of all strategies involving vegetation (i.e., scenarios 1 + 2 + 3); 5) high-albedo roofs; and 6) high-albedo surfaces, including roofs, sidewalks, and roadways (i.e., scenario 5 + sidewalks and roadways). Each scenario assumed that the mitigation strategy was implemented in all of the available area within the case study. This means that different amounts of

[6] This dataset is a proxy for vegetation fraction intensity, because it actually represents the fractional area of a pixel that is vegetated and not the intensity of the vegetated area. Also, the values represent only illuminated vegetation, not actual vegetation, because optical satellite sensors can only measure reflected light.

Table 1. Parameters for land surface cover types used in MM5 simulations of New York City. The three types of cover—impervious, grass, and trees—are represented as tiles within 1.3-km MM5 grid cells.

Model parameter	Impervious	Grass	Trees
Leaf area index	0.0	1	6
Vegetation fraction intensity	0.0	0.5	0.9
Minimum canopy resistance (s m^{-1})	n/a	40	100
Shortwave albedo (%)	15	19	16
Longwave emissivity (%)	88*	98.5	93
Local roughness length (cm)	5	12	50
Initial soil moisture** (% of saturation)	All layers 0%	Top layer 50%; others 90%	All layers 90%

* Standard USGS value for impervious surfaces in MM5 land-use module.

** To initialize the model, we assumed that soils were wet. Because soils are often dry throughout a heat wave, this may have introduced a small error into our results.

surface cover were altered in different case study neighborhoods (Table 2). Surface cover alterations were simulated based on the MM5 tile calculations and the base percent of each land surface cover type in each grid cell. We do not model the height of each intervention. Therefore, an important caveat is the assumption that grass planted on rooftops has the same effect as grass planted at street level, or elsewhere within the urban canopy.

In scenarios involving tree planting, tiles representing grass and/or impervious surfaces were changed to trees, and all trees were assumed to be deciduous and mature at the time of planting. This approach simulates pockets of closed-canopy forest within an urban setting. In reality, trees shade built surfaces, with gaps that expose underlying surfaces to solar radiation. We also assume that evapotranspiration is the only mechanism through which trees cool the urban environment because of the difficulty in simulating energy fluxes beneath a tree canopy within MM5. Finally, it was assumed that there was sufficient rainfall prior to each heat wave such that transpiration was not constrained.

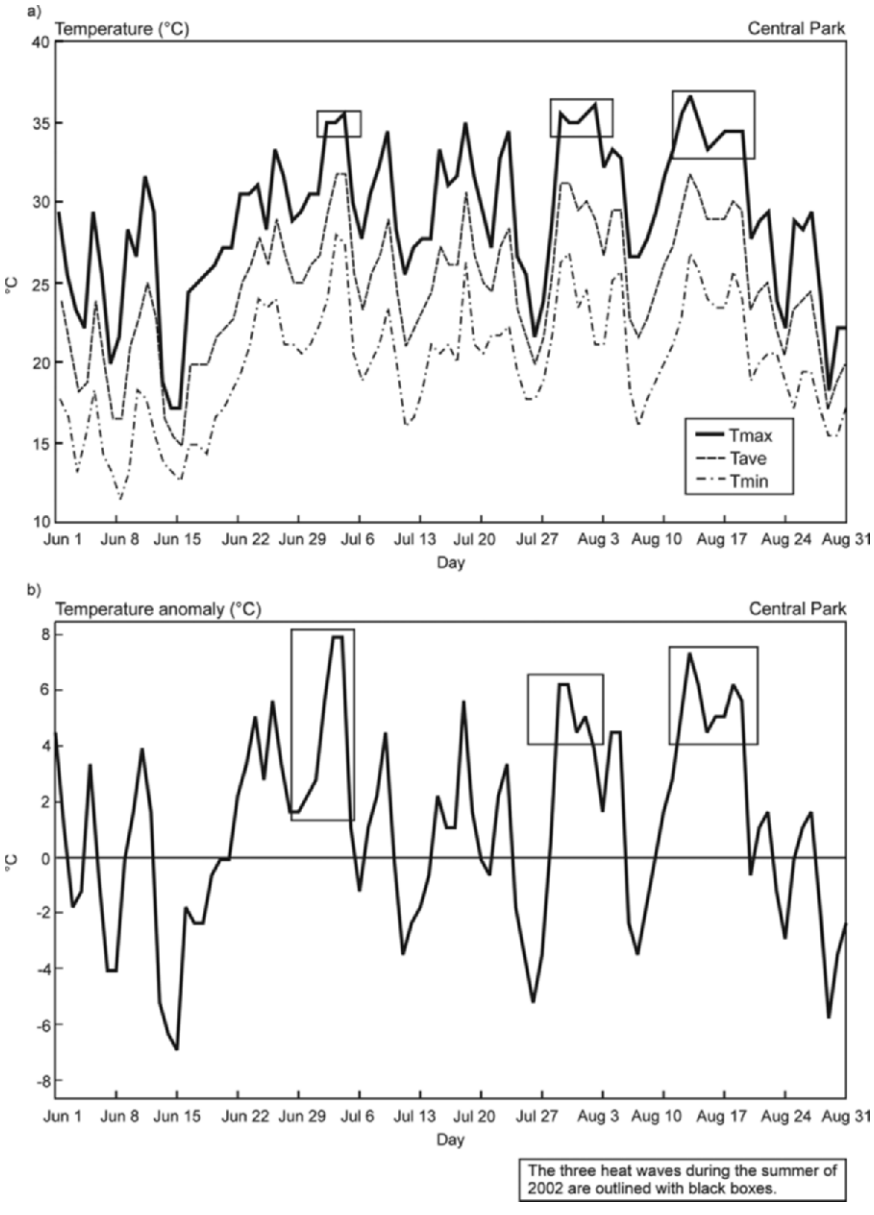

Fig. 5. Observed surface air temperature and heat-wave days from the Central Park NWS station, 1 Jun–31 Aug 2002. (a) Maximum, minimum, and mean surface air temperature. (b) Surface air temperature anomaly. Note: A heat wave is defined as three consecutive days with maximum surface air temperature >32.2°C.

Following Bass et al. (2003), green roof vegetation was modeled as grass, and was assumed to function in the same way as grass planted at street level. Because roof surfaces tend to be hotter than impervious street-level surfaces, rooftop grass would be expected to have a greater cooling effect on radiative surface temperature than street-level grass. However, the ambient air temperature tends to be cooler at the top of the urban canyon, where rooftops are located, so that the impact of green roofs on urban air temperature may be reduced. Also, because most urban green roof systems use a thin layer of lightweight growing medium to support drought-resistant plants, evapotranspiration may be lower than for grass, particularly for common green roof plants that transpire at night (e.g., sedums).

In scenarios involving high-albedo surfaces, the commercial availability of different materials for rooftop versus street-level application was considered. An albedo of 0.5 was chosen for rooftops, and 0.2 was chosen for roadways and pavements. On rooftops, new bright white coatings can have an albedo greater than 0.5 (as opposed to an estimated average albedo of 0.15

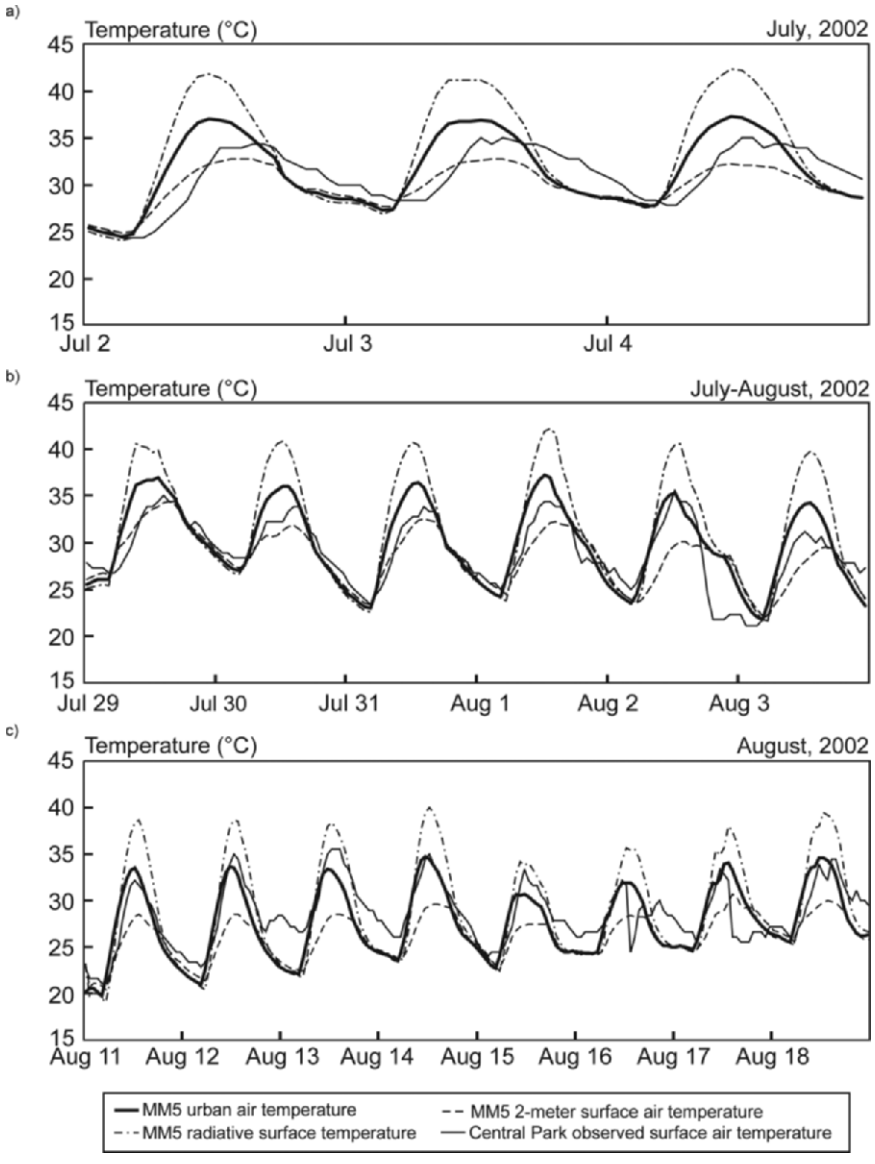

Fig. 6. Evaluation of MM5 urban air temperature against observed mean surface air temperature from Central Park for each summer heat-wave period, 2002. MM5-simulated 2-m air temperature and radiative surface temperature are also shown. (a) 2–4 Jul heat wave. (b) 29 Jul–3 Aug heat wave. (c) 11–18 Aug heat wave.

for impervious surfaces in New York City), but the coatings fade over time because of weather, staining, and soot deposition (Heat Island Group 2006). On roadways, asphalt pavement typically consists of 7/8 volume rock aggregate bound by 1/8 volume dark asphalt (bitumen), with a very low albedo. In New York, high-albedo aggregate is widely available, but high-albedo binder remains experimental, limiting the achievable increase in albedo to an estimated 0.2.

RESULTS AND DISCUSSION. Based on simulations with MM5, we found that small reductions in New York City's urban air temperature can be achieved by implementing heat island mitigation strategies (Table 3). Results indicate that the influence of vegetation on urban climate is more important than the influence of the albedo of built surfaces. The most effective way to reduce urban air temperature is to maximize the amount of vegetation in the city with a combination of tree planting and green roofs. Applying this strategy reduced simulated citywide urban air temperature by 0.4°C on average, and 0.7°C at 1500 EST, a time of day that corresponds to the peak commercial electricity load. Simulated reductions of up to 1.1°C at 1500 EST occurred in some neighborhoods in Manhattan and Brooklyn, primarily because there is more available area in which to plant trees and install vegetated roofs in these boroughs. In Manhattan, most of the mitigation would involve greening rooftops high above the street, whereas in Brooklyn, a more balanced combination of the two strategies could be employed.

Modeling studies of urban heat island mitigation in several different cities with strongly differing urban geometries show a range of effectiveness averaged over all times of day on the order of 0.2°–3.6°C (Taha et al. 1999; Luley and Bond 2002; Bass et al. 2003). Results from this study fall at the lower end of the range primarily because of the relatively large amount of built surfaces, the relative paucity of area available for mitigation after accounting for infrastructure constraints, and the strong presence of land–sea interactions that generate sea breezes across much of the city.

Our results may also have been affected by cool biases (i.e., modeled air temperatures that are con-

Table 2. Heat island mitigation scenarios simulated with MM5 by altering the percentage of impervious, grass, and tree-covered land surfaces in each case study area. Each scenario assumes implementation of the strategy in 100% of the available area within that case study neighborhood. Data are shown as impervious (%), grass (%), trees (%) rounded to the nearest whole number, with high-albedo percentages appearing as a fourth number as applicable. For example, in the New York City high-albedo roofs scenario, 51% of the land surface cover is composed of existing impervious surfaces, 14% is grass, 22% is trees, and 14% is high-albedo impervious surface. In the open-space tree-planting scenario, it was assumed that any area that is currently grassy could be planted with trees unless it had been delineated as a cemetery, ball field, playground, garden, or tennis courts. In the green roof and high-albedo roof scenarios, available area is based on altering 75% of the total flat roof area, with New York City roof data derived by aggregating all residential, commercial, and industrial land-use classes likely to have flat roof architecture. The remaining 25% of the total flat roof area is assumed to be unavailable because of rooftop infrastructure conflicts and building codes requiring a nongreened border on each roof.

Case study	Base	Increased vegetation				High albedo	
		Trees in open space	Street trees	Green roofs	Combined	High-albedo roofs	High-albedo surfaces
	Impervious (%), grass (%), trees (%), high albedo (%)						
New York City	64, 14, 22	64, 3, 33	57, 14, 29	51, 28, 22	44, 17, 39	51, 14, 22, 14	16, 14, 22, 48
Mid-Manhattan West	94, 3, 3	94, 1, 5	86, 3, 11	61, 36, 3	53, 35, 13	61, 3, 3, 34	24, 3, 3, 71
Lower Manhattan East	84, 8, 8	84, 3, 14	75, 8, 17	57, 35, 8	48, 29, 23	57, 8, 8, 27	21, 8, 8, 63
Fordham Bronx	69, 9, 22	69, 1, 31	59, 9, 32	53, 25, 22	43, 17, 41	53, 9, 22, 16	17, 9, 22, 51
Maspeth Queens	60, 18, 22	60, 2, 38	54, 18, 29	44, 34, 22	38, 18, 44	44, 18, 22, 17	15, 18, 22, 45
Crown Heights	75, 8, 17	75, 0, 25	60, 8, 32	53, 30, 17	39, 22, 39	53, 8, 17, 22	19, 8, 17, 56
Ocean Parkway	80, 6, 15	80, 0, 20	66, 6, 28	58, 27, 15	45, 22, 33	58, 6, 15, 22	20, 6, 15, 60

Table 3. Changes in urban air temperature (°C) based on MM5 simulations. Results at top are averaged over all 17 heat-wave days and all grid cells representing each case study. Results are shown below for 1500 EST both because the greatest temperature reductions tend to occur in midafternoon, and because this time of day corresponds with commercial peak electricity demand in the summer. Results across strategies and case studies are significantly different from one another at the 0.05 level, with the exception of results for street trees and green roofs in Crown Heights Brooklyn.

Case study neighborhood	Increased vegetation				High albedo	
	Trees in open space	Street trees	Green roofs	Combined	High-albedo roofs	High-albedo surfaces
Average 1500 EST reduction (°C)						
New York City	−0.1	−0.1	−0.2	−0.4	−0.2	−0.2
Mid-Manhattan West	0.0	−0.2	−0.5	−0.6	−0.3	−0.4
Lower Manhattan East	−0.1	−0.2	−0.4	−0.6	−0.3	−0.3
Fordham Bronx	−0.1	−0.2	−0.2	−0.4	−0.2	−0.2
Maspeth Queens	−0.1	−0.1	−0.2	−0.4	−0.2	−0.2
Crown Heights Brooklyn	−0.1	−0.3	−0.3	−0.7	−0.2	−0.3
Average 1500 EST reduction (°C)						
New York City	−0.1	−0.2	−0.3	−0.7	−0.3	−0.3
Mid-Manhattan West	0.0	−0.3	−0.8	−1.1	−0.6	−0.7
Lower Manhattan East	−0.1	−0.3	−0.6	−1.0	−0.5	−0.6
Fordham Bronx	−0.1	−0.3	−0.4	−0.7	−0.3	−0.3
Maspeth Queens	−0.2	−0.2	−0.4	−0.8	−0.3	−0.4
Crown Heights Brooklyn	−0.1	−0.5	−0.5	−1.1	−0.4	−0.5
Ocean Parkway Brooklyn	−0.1	−0.5	−0.6	−1.1	−0.4	−0.6

sistently lower than observed air temperatures) that have been reported in applications of MM5 to urban settings (Zhender 2002). These were diagnosed as resulting from the parameterizations for building effects on low-level circulation and temperature gradients, and also the ground-level energy balance fluxes. Other urban simulations have reported similar issues (Martilli et al. 2003; Dandou et al. 2005). Given the vast heterogeneous and structural composition of urban surfaces, superimposed with dynamic anthropogenic activities, such shortcomings are to be expected. This is especially true in New York City, with its particularly dense urban structure surrounded by water.

We carefully analyzed the amount of available area for each of the mitigation strategies because this is a key constraint as well as a driver of differences across strategies and neighborhoods. We found that, although planting street trees citywide has only half the impact of high-albedo surfaces, it involves planting trees in 7% of the city's area, as compared to raising the albedo of 48% of the city's surfaces. This signals the need to compare strategies on a per-unit-area basis. To do this for the street-tree strategy, for example, we computed the average urban air temperature of all tiles representing trees and subtracted this from the average urban air temperature of all tiles representing impervious surfaces. The number of tiles representing each land surface cover type in the per-unit-area analysis was the same as the number of MM5 grid cells representing New York City because each tile represents a single land surface cover type within each grid cell. In the street-tree case, we estimated an average difference in urban air temperature of 1.9°C across all heat-wave days and times of day. Because the corresponding result for high-albedo roofs and surfaces was 1.1°C, our results show that street trees provide approximately 72% more cooling per unit area, on average (Table 4). In other words, changing a given area of impervious surface to trees provides 72% more cooling than changing that same area to a high-albedo surface. Another way to interpret the results in Table 4 is as an upper bound. For example, if all impervious surface area is changed to trees regardless of the amount of area available for redevelopment, then the total urban air temperature reduction is expected to be 1.9°C.

Furthermore, because regional climate models have not yet been fully parameterized for complex urban environments at very fine resolutions (i.e., <4 km), there is greater certainty in the relative predictions across strategies and neighborhoods than in the magnitude of the predictions. Complex urban sites such as New York City require continuing research to estimate key mesoscale modeling parameters (roughness lengths, thermal conductivities and capacities, and boundary layer representations) to better simulate urban microclimate.

IMPACTS ON ELECTRICITY DEMAND. The impact of heat island mitigation on electricity demand was estimated using simple statistical models that relate electric load to surface air temperature. Con Edison provided electricity consumption data for each neighborhood and heat wave included in the study. Results of the electricity demand analysis were used in a cost–benefit analysis of each strategy. Only energy benefits were considered. We summarize the preliminary results based on these analyses. Note that variations in electric load are due to many factors not incorporated into the statistical models, including ambient weather conditions, building occupancy

Table 4. Average and maximum differences in urban air temperature simulated with MM5. Average differences were computed over all grid cells and heat-wave days and times and rounded to one decimal place. The maximum is the largest temperature difference in any grid cell at any hour on any of the heat-wave days. Each value is the difference between the temperature of the warmer land surface cover type and the cooler land surface cover type. For example, the simulated urban air temperature associated with tiles representing trees is on average 0.6°C cooler then the urban air temperature associated with tiles representing grass. Because the average difference between impervious surface and trees is 1.9°C, this implies that planting street trees is approximately 3 times as effective per unit area as planting trees in open space.

Difference between land surface types	Relevant mitigation strategy	Average (°C) (over all grid cells and times of day)	Maximum (°C) (in any grid cell at any time of day)
Grass minus trees	Trees in open space	0.6	1.7
Impervious minus trees	Street trees	1.9	4.8
Impervious minus grass	Green roofs	1.4	3.2
Impervious minus high albedo	High-albedo roofs and surfaces	1.1	2.6

patterns (time of day and day of week), and load distribution among users.

Our initial findings indicate the possibility of small reductions (<1%) in peak electric load for individual mitigation strategies. Of the six case studies, there are no neighborhoods where individual mitigation strategies are expected to reduce peak electric load by more than 1%, although a combined strategy of tree planting and green roofs is associated with peak load reductions of 2%–3%, depending on the neighborhood (Rosenzweig et al. 2006b).

If the combined strategy is implemented across the city, the benefit in terms of avoided power generation, and using wholesale electric rates, is estimated at more than $1 billion over the 35-yr estimated lifetime of a heat island mitigation strategy. This assumes a fully mature mitigation strategy at the beginning of the 35-yr period.

Urban heat island mitigation strategies involving vegetation tend to be more expensive per unit area than strategies involving high-albedo surfaces. The cost–benefit analysis indicates that, after considering costs, high-albedo surfaces may be a more cost-effective way to reduce electricity demand when compared with tree planting or green roofs. However, incorporating other benefits, including air quality and public health improvements, and reductions in the city's stormwater runoff and contribution to greenhouse gas emissions would likely improve the cost effectiveness of strategies involving vegetation.

POLICY OUTCOMES AND RECOMMENDATIONS. Stakeholders involved in the project targeted some of the neighborhoods identified in this study for tree-planting programs. For example, study findings guided a $400,000 pilot tree-planting project in Lower Manhattan and are informing a $10 million tree-planting program in the Bronx sponsored by NYSERDA and the NYSDEC. Project results helped stakeholders identify criteria to include in their funding announcements for community-based tree-planting programs.

As part of follow-up research, we collected detailed field data on surface air temperature and radiative surface temperature along shaded and unshaded streets in these neighborhoods. With colleagues in the metropolitan region, we are also developing the Urban Ocean-Atmosphere Observatory to provide the needed detailed data for calibration of urbanized regional climate models. Such data can also help stakeholders better understand on-the-ground conditions in each neighborhood as they prepare programs for implementation.

Recommendations based on the integration of stakeholder perspectives and scientific knowledge include the following:

1) Develop urban heat island mitigation strategies appropriate to priorities and conditions in individual neighborhoods and communities.
2) Maximize the temperature impact of urban heat island mitigation through combination strategies, and particularly by planting trees along streets and in open spaces, as well as installing green roofs.
3) Monitor tree-planting programs, green roofs, and high-albedo surfaces to document actual mitigation levels over time and use results to improve the design of future heat island mitigation programs.
4) Conduct additional analyses to value energy benefits of the mitigation scenarios, and include other benefits of mitigation strategies, such as air quality, public health, stormwater runoff, and reduction of greenhouse gas emissions, in cost–benefit analyses.

ACKNOWLEDGMENTS. This project was funded by NYSERDA as part of two New York Energy $mart programs, the Peak Load Reduction Program (PLRP), and the Environmental Monitoring, Evaluation, and Protection (EMEP) program. Funding support was also provided by the U.S. Department of Agriculture, Forest Service, in collaboration with the New York State Department of Environmental Conservation (DEC). We are grateful to the reviewers for constructive comments that improved the paper greatly. We thank José Mendoza for graphical support.

APPENDIX: DATASETS INCLUDED IN PROJECT DATA LIBRARY.

Dataset	Description
Landsat-7 Enhanced Thematic Mapper (ETM) + 22 Jul, 14 Aug, 8 Sep 2002	1030 EST; visible and near-infrared bands spatial resolution is 30 m; thermal infrared band spatial resolution is 60 m
Advanced Spaceborne Thermal Emission and Reflection Radiometer (ASTER) 8 Sep 2002	1030 EST; spatial resolution is 90 m
Moderate Resolution Imaging Spectroradiometer (MODIS) day–night pair 8 Sep 2002	1030 and 2230 EST; spatial resolution is 1 km

Dataset	Description
Normalized difference vegetation index (NDVI)	Calculated using visible and near-infrared Landsat data; spatial resolution is 30 m
Albedo	Integrated measure of reflected radiance at visible to near-infrared wavelengths calculated by Small (2003); spatial resolution is 30 m
Road density	Calculated using U.S. Census TIGER* 2002 roads data; total road kilometers aggregated to 60-m grid cells
Building height	Number of building stories in each tax parcel extracted from the 2002 real property database of New York City's Department of Finance
Building floor area	Area of each tax parcel based on the 2002 real property database of New York City's Department of Finance
Year built	Year of construction based on the 2002 real property database of New York City's Department of Finance
Population density	Calculated based on U.S. Census 2000 data for block groups
Land surface cover	Classification into impervious, grass, trees, and water by Myeong et al. (2001); spatial resolution is 3 m
Street trees	Based on GIS layer created by the New York City Department of Parks and Recreation; to convert line-segment data to areas, a canopy area of 104 m^2 per tree was assumed based on deciduous, mature trees (J. Lu 2005, personal communication); existing trees subtracted from the hypothetical maximum carrying capacity for each street

*Topologically Integrated Geographic Encoding and Referencing System.

Note: Land surface data used in MM5 simulations were aggregated to 1.3-km MM5 grid cells.

REFERENCES

Aniello, C., K. Morgan, A. Busbey, and L. Newland, 1995: Mapping micro-urban heat islands using Landsat TM and a GIS. *Comput. Geosci.,* **21,** 965–969.

Arnfield, A., 2003: Two decades of urban climate research: A review of turbulence, exchanges of energy and water, and the urban heat island. *Int. J. Climatol.,* **23,** 1–26.

Bass, B., E. S. Krayenhoff, A. Martilli, R. B. Stull, and H. Auld, 2003: The impact of green roofs on Toronto's urban heat island. *Proc. First North American Green Roof Conference: Greening Rooftops for Sustainable Communities,* Chicago, IL, Toronto (Canada) Cardinal Group, 292–304.

Bretz, S., and B. Pon, 1994: Durability of high albedo coatings. *Recent Research in the Building and Energy Analysis Group at Lawrence Berkeley Laboratory,* No. 5, Building Energy Analysis Group, p. 1. [Available online at http://eetd.lbl.gov/Buildings/RResearch/Albedo.html.]

Brown, J. E., T. R. Loveland, J. W. Merchant, B. C. Reed, and D. O. Ohlen, 1993: Using multi-source data in global land-cover characterization: Concepts, requirements, and methods. *Photogram. Eng. Remote Sens.,* **59,** 977–987.

Chen, F., and J. Dudhia, 2001a: Coupling an advanced land-surface/hydrology model with the Penn State/NCAR MM5 modeling system. Part I: Model implementation and sensitivity. *Mon. Wea. Rev.,* **129,** 569–585.

——, and ——, 2001b: Coupling an advanced land-surface/hydrology model with the Penn State/NCAR MM5 modeling system. Part II: Preliminary model validation. *Mon. Wea. Rev.,* **129,** 587–604.

Childs, P. P., and S. Raman, 2005: Observations and numerical simulations of urban heat island and sea breeze circulations over New York City. *Pure Appl. Geophys.,* **162,** 1955–1980.

Civerolo, K., G. Sistla, S. T. Rao, and D. J. Nowak, 2000: The effects of land use in meteorological modeling: Implications for assessment of future air quality scenarios. *Atmos. Environ.,* **34,** 1615–1621.

Dandou, A., M. Tombrou, E. Akylas, N. Soulakellis, and E. Bossioli, 2005: Development and evaluation of an urban parameterization scheme in the Penn State/NCAR Mesoscale Model (MM5). *J. Geophys. Res.,* **110,** D10102, doi:10.1029/2004JD005192.

Davis, S., P. Martien, and N. Sampson, 1992: Planting and light-colored surfacing for energy conservation.

Cooling our Communities: A guidebook on tree planting and light-colored surfacing, H. Akbari et al., Eds., United States Environmental Protection Agency, 93–110.

Dudhia, J., 1993: A nonhydrostatic version of the Penn State/NCAR mesoscale model: Validation tests and simulation of an Atlantic cyclone and cold front. *Mon. Wea. Rev.,* **121,** 1493–1513.

Gaffin, S. R., and Coauthors, 2008: Variations in New York City's urban heat island strength over time and space. *Theor. Appl. Climatol.,* **94,** 1–11.

Gedzelman, S. D., S. Austin, R. Cermak, N. Stefano, S. Partridge, S. Quesenberry, and D. A. Robinson, 2003: Mesoscale aspects of the urban heat island around New York City. *Theor. Appl. Climatol.,* **75,** 29–42.

Grell, G. A., Dudhia, J., and D. R. Stauffer, 1995: A description of the fifth-generation Penn State/NCAR mesoscale model (MM5). NCAR Tech. Note NCAR/TN-398+STR, 122 pp.

Grimmond, C. S. B., 2007: Urbanization and global environmental change: Local effects of urban warming. *Geogr. J.,* **173,** 83–88.

——, and T. R. Oke, 1999: Heat storage in urban areas: Local-scale observations and evaluation of a simple model. *J. Appl. Meteor.,* **38,** 922–940.

Heat Island Group, cited 2006: Pavement albedo. [Available online at http://eetd.lbl.gov/heatisland/Pavements/Albedo/.]

Hogrefe, C., and Coauthors, 2004: Simulating changes in regional air pollution over the eastern United States due to changes in global and regional air pollution over the eastern United States due to changes in global and regional climate and emissions. *J. Geophys. Res.,* **109,** D22301, doi:10.1029/2004JD004690.

Hsieh, C. M., T. Aramaki, and K. Hanaki, 2007: The feedback of heat rejection to air conditioning load during the nighttime in subtropical climate. *Energy Build.,* **39,** 1175–1182.

Kirkpatrick, J. S., and M. D. Shulman, 1987: A statistical evaluation of the New York City–northern New Jersey urban heat island effect on summer daily minimum temperature. *Natl. Wea. Dig.,* **12,** 12.

Landsberg, C., 1981: *The Urban Climate*. Academic Press, 275 pp.

Levinson, R., H. Akbari, and J. C. Reilly, 2007: Cooler tile-roofed buildings with near-infrared-reflective non-white coatings. *Build. Environ.,* **42,** 2591–2605.

Liu, Y., F. Chen, T. Warner, and J. Basara, 2006: Verification of a mesoscale data-assimilation and forecasting system for the Oklahoma City area during the Joint Urban 2003 Field Project. *J. Appl. Meteor. Climatol.,* **45,** 912–929.

Luley, C. J., and J. Bond, 2002: A plan to integrate management of urban trees into air quality planning: A report to the Northeast State Foresters Association. 61 pp. [Available online www.fs.fed.us/ne/syracuse/Pubs/Downloads/Final_report_March2002_Davey.pdf.]

Lynn, B., and Coauthors, 2009: A modification to the Noah LSM to simulate heat mitigation strategies in the New York City metropolitan area. *J. Appl. Meteor. Climatol.,* **48,** 199–216.

Martilli, A., Y.-A. Roulet, M. Junier, F. Kirchner, M. W. Rotach, and A. Clappier, 2003: On the impact of urban surface exchange parameterizations on air quality simulations: The Athens case. *Atmos. Environ.,* **37,** 4217–4231.

Myeong, S., D. J. Nowak, P. F. Hopkins, and R. H. Brock, 2001: Urban cover mapping using digital, high-spatial resolution aerial imagery. *Urban Ecosyst.,* **5,** 243–256.

New York City Office of Emergency Management, cited 2008: NYC hazards: Extreme heat basics. [Available online at www.nyc.gov/html/oem/html/hazards/heat_basics.shtml.]

Nowak, D. J., K. L. Civerolo, S. Trivikrama Rao, G. Sistla, C. J. Luley, and D. E. Crane, 2000: A modeling study of the impact of urban trees on ozone. *Atmos. Environ.,* **34,** 1601–1613.

OASIS, cited 2001: Classified landcover (2001). NYC OASIS. [Available online at www.oasisnyc.net/metadata.asp?CLN=LANDCOVER.]

Oke, T. R., 1981: Canyon geometry and the nocturnal urban heat island: Comparison of scale model and field observations. *J. Climatol.,* **1,** 237–254.

——, 1987: *Boundary Layer Climates*. 2nd ed. Routledge Press, 435 pp.

——, 2006: Towards better scientific communication in urban climate. *Theor. Appl. Climatol.,* **84,** 179–190.

Otte, T. L., A. Lacser, S. Dupont, and J. K. S. Ching, 2004: Implementation of an urban canopy parameterization in a mesoscale meteorological model. *J. Appl. Meteor.,* **43,** 1648–1665.

Pielke, R. A., 2001: *Mesoscale Meteorological Modeling*. Academic Press, 676 pp.

Rosenfeld, A. H., H. Akbari, S. Bretz, B. L. Fishman, D. M. Kurn, D. Sailor, and H. Taha, 1995: Mitigation of urban heat island: Materials, utility programs, updates. *Energy Build.,* **22,** 255–265.

Rosenthal, J., M. Pena Sastre, C. Rosenzweig, K. Knowlton, R. Goldberg, and P. Kinney, 2003: One hundred years of New York City's "urban heat island": Temperature trends and public health impacts. *Eos, Trans. Amer. Geophys. Union,* **84,** (Fall Meeting Suppl.), Abstract U32A-0030.

Rosenzweig, C., W. D. Solecki, L. Parshall, M. Chopping, G. Pope, and R. Goldberg, 2005: Characterizing the urban heat island effect in current and future climates in urban New Jersey. *Environ. Hazards,* **6,** 51–62.

——, S. Gaffin, and L. Parshall, 2006a: Green roofs in the New York metropolitan region: Research report. NASA/Goddard Institute for Space Studies and Columbia Center for Climate Systems Research of the Earth Institute at Columbia University, 59 pp.

——, W. D. Solecki, and R. B. Slosberg, 2006b: Mitigating New York City's heat island with urban forestry, living roofs, and light surfaces. NYSERDA Rep. 06-06, 133 pp.

Sailor, D., L. S. Kalkstein, and E. Wong, 2002: Alleviating heat-related mortality through urban heat island mitigation. *Bull. Amer. Meteor. Soc.,* **83,** 663–664.

Small, C., 2001: Estimation of urban vegetation abundance by spectral mixture analysis. *Int. J. Remote Sens.,* **22,** 1305–1334.

——, 2003: High spatial resolution spectral mixture analysis of urban reflectance. *Remote Sens. Environ.,* **88,** 170–186.

Taha, H., 1996: Modeling impacts of increased urban vegetation on ozone air quality in the south coast air basin. *Atmos. Environ.,* **30,** 3423–3430.

——, 1997: Urban climates and heat islands: Albedo, evapotranspiration and anthropogenic heat. *Energy Build.,* **25,** 99–103.

——, S. Douglas, and J. Haney, 1997: Mesoscale meteorological and air quality impacts of increased urban albedo and vegetation. *Energy Build.,* **25,** 169–177.

——, W. Konopacki, and S. Gabersek, 1999: Impacts of large-scale surface modifications on meteorological conditions and energy use: A 10-region modeling study. *Theor. Appl. Climatol.,* **62,** 175–185.

Unwin, D. J., 1980: The synoptic climatology of Birmingham's urban heat island. *Weather,* **35,** 43–50.

U.S. EPA, cited 2007: Heat island reduction initiative—Research. [Available online at www.epa.gov/heatisland/research/index.html.]

Voogt, J. A., and T. R. Oke, 2003: Thermal remote sensing of urban areas. *Remote Sens. Environ.,* **86,** 370–384.

Zehnder, J. A., 2002: Simple modifications to improve fifth-generation Pennsylvania University–National Center for Atmospheric Research Mesoscale Model performance for the Phoenix, Arizona, metropolitan area. *J. Appl. Meteor.,* **41,** 971–979.